

A Class of Quadrature-Based Moment-Closure Methods with Application to the Vlasov-Poisson-Fokker-Planck System in the High-Field Limit

Yongtao Cheng^a, James A. Rossmanith^{b,1}

^aUniversity of Wisconsin, Department of Mathematics, 480 Lincoln Drive, Madison, WI 53706, USA

^bIowa State University, Department of Mathematics, 396 Carver Hall, Ames, IA 50011, USA

Abstract

Quadrature-based moment-closure methods are a class of approximations that replace high-dimensional kinetic descriptions with lower-dimensional fluid models. In this work we investigate some of the properties of a sub-class of these methods based on bi-delta, bi-Gaussian, and bi-B-spline representations. We develop a high-order discontinuous Galerkin (DG) scheme to solve the resulting fluid systems. Finally, via this high-order DG scheme and Strang operator splitting to handle the collision term, we simulate the fluid-closure models in the context of the Vlasov-Poisson-Fokker-Planck system in the high-field limit. We demonstrate numerically that the proposed scheme is asymptotic-preserving in the high-field limit.

Keywords: Asymptotic-Preserving; Discontinuous Galerkin; Vlasov-Poisson; Fokker-Planck; Moment-Closure; Moment-Realizability; Plasma Physics; High-Order Schemes

1. Introduction

The focus of this work is on 1D fluid models of plasma with a class of fluid-closure approximations known as *quadrature-based moment-closures*. In particular, in this work we are interested in applying these fluid-closure approximations to the one-dimensional form the Vlasov-Poisson-Fokker-Planck (VPFP) equations:

$$\tilde{f}_{,\tilde{t}} + \tilde{v}\tilde{f}_{,\tilde{x}} - \frac{e}{m}\tilde{E}\tilde{f}_{,\tilde{v}} = \mu \left(\tilde{v}\tilde{f} + \frac{k_B\Theta}{m}\tilde{f}_{,\tilde{v}} \right)_{,\tilde{v}}, \quad \tilde{E}_{,\tilde{x}} = \frac{e}{m\epsilon_0}(\tilde{\rho}_0 - \tilde{\rho}), \quad (1)$$

Email addresses: cheng@math.wisc.edu (Yongtao Cheng), rossmani@iastate.edu (James A. Rossmanith)

¹Corresponding author

where $\tilde{t} \in \mathbb{R}$ is time, $\tilde{x} \in \mathbb{R}$ is the spatial coordinate, $\tilde{v} \in \mathbb{R}$ is the velocity, $\tilde{f}(\tilde{t}, \tilde{x}, \tilde{v})$ is the probability density function for electrons, $\tilde{E}(\tilde{t}, \tilde{x})$ is the electric field, and $\tilde{\rho} = \int m \tilde{f} d\tilde{v}$ is the electron mass density. The parameters in this equation are the elementary charge, e , the electron mass, m , the Boltzmann constant, k_B , the temperature of the equilibrium state, Θ , and the stationary background ion mass density, $\tilde{\rho}_0(\tilde{x})$. In the above expression $\tilde{\cdot}$ is used to denote dimensional dependent and independent variables (i.e., these decorations will be removed after non-dimensionalization). These equations describe the dynamics of electrons (as represented by the PDF $\tilde{f}(\tilde{t}, \tilde{x}, \tilde{v})$) that evolve via Coulomb interactions and collisions in the form of a Fokker-Planck drift-diffusion operator. The Fokker-Planck operator tries to drive the system to a thermodynamic equilibrium with constant temperature Θ .

1.1. The Vlasov-Poisson-Fokker-Planck system in the high-field limit

Fluid-closure methods as described in this work will generally not accurately approximate solutions of (1) in the collisionless limit, $\varepsilon \rightarrow \infty$. Instead, we focus here on the high-collision limit; and in particular, the *high-field limit*, which describes the long-time, large-scale, high-collisional, and large electric field limit of the VPFP system.

In order to derive the high-field limit of the VPFP system we introduce a non-dimensionalization via the characteristic scaling constants: T (time), L (length), E_0 (electric field), and N (number density), such that

$$\tilde{t} = Tt, \quad \tilde{x} = Lx, \quad \tilde{v} = LT^{-1}v, \quad \tilde{E} = E_0E, \quad \tilde{\rho} = mN\rho, \quad \tilde{f} = NTL^{-1}f.$$

This reduces the VPFP system (1) to

$$f_{,t} + vf_{,x} - \mu T \left(\frac{eE_0T}{\mu m L} \right) Ef_{,v} = \mu T \left(vf + \left(\frac{k_B T^2 \Theta}{m L^2} \right) f_{,v} \right)_{,v}, \quad E_{,x} = \left(\frac{eLN}{\epsilon_0 E_0} \right) (\rho_0 - \rho).$$

We define the dimensionless parameter $\varepsilon = (\mu T)^{-1}$ and choose T , L , and E_0 as follows:

$$T = \frac{m\epsilon_0\mu}{Ne^2}, \quad L = \sqrt{mk_B\Theta} \left(\frac{\epsilon_0\mu}{Ne^2} \right), \quad E_0 = \frac{\mu}{e} \sqrt{mk_B\Theta}. \quad (2)$$

After simplification, this results in the following non-dimensional Vlasov-Poisson Fokker-Planck (VPFP) system:

$$f_{,t} + vf_{,x} = \frac{1}{\varepsilon} \left(F(F^{-1}f)_{,v} \right)_{,v}, \quad E_{,x} = \rho_0 - \rho, \quad (3)$$

where $\rho = \int f dv$ and $F(t, x, v)$ is the isothermal equilibrium distribution:

$$F(t, x, v) = \frac{\rho(t, x)}{\sqrt{2\pi}} \exp \left(-\frac{1}{2} (v + E(t, x))^2 \right). \quad (4)$$

The so-called *high-field limit* is when $\varepsilon \rightarrow 0^+$, which, under the choices of the characteristic time, length, and electric field chosen in (2), describes long time

($T \rightarrow \infty$), large-scale ($L \rightarrow \infty$), and large electric field ($E_0 \rightarrow \infty$) dynamics of the VPFP system. In particular, Nieto et al. [20] proved that as $\varepsilon \rightarrow 0^+$, the solution of the VPFP system (3) converges to the equilibrium distribution (4), where (to leading order in ε) the mass density, $\rho(t, x)$, and the electric field, $E(t, x)$, satisfy the following non-local advection equation:

$$\rho_{,t} - (\rho E)_{,x} = 0, \quad E_{,x} = \rho_0 - \rho. \quad (5)$$

1.2. Scope of this work

Recently, Wang and Jin [14] developed an *asymptotic-preserving* scheme for the VPFP equation, where they modified a fully kinetic solver for VPFP so that it remains asymptotic preserving in the high-field limit $\varepsilon \rightarrow 0^+$. The approach has the nice property that it can be applied for *any* value of $\varepsilon > 0$. The problem with the Wang and Jin [14] scheme is that if one is really interested in regimes where ε is relatively small (i.e., *near* thermodynamic equilibrium), then their approach is computationally expensive (i.e., requires solving a PDE in 2D rather than 1D).

The purpose of this work is to consider fluid models for the VPFP system that not only have the ability to capture the equilibrium dynamics of VPFP (i.e., equation (5)), but also accurately model near-equilibrium dynamics. The scope of the current work is to twofold:

1. We describe and investigate properties of two approaches in the quadrature-based moment-closure framework as developed in Fox [10] (bi-delta distribution functions) and Chalons, Fox, and Massot [5] (bi-Gaussian distribution functions), and describe a modification of these based on bi-B-spline distributions. This is described in §2.
2. We then take this class of quadrature-based moment-closure approaches and, via a high-order discontinuous Galerkin scheme with Strang operator splitting for the collision operator, approximately solve the VPFP system in the high-field limit. The numerical method is developed in §3 and applied to two test problems from Wang and Jin [14] in §4.

2. Quadrature-based moment-closure methods

In this section we describe three variants of the quadrature-based moment-closure approach. In §2.1 we describe the simplest of these: quadrature based on delta distributions. Delta distributions have been used in several previous works including in gas dynamics applications in Fox [10] and Yan and Fox [25], multivalued solutions of Euler-Poisson [17], and multiphase solutions of the semiclassical limit of the Schrödinger equation [11, 13]. In §2.2 we describe a generalization of this approach using Gaussian distributions developed by Chalons, Fox, and Massot [5]. Finally in §2.3 we propose a modification of the Gaussian distribution approach that uses compactly supported B-splines.

2.1. Quadrature using delta distributions

In the quadrature-based moment-closure approach using delta distributions we assume a PDF that is a sum of delta functions with unknown weights and positions (we show here the simplest version of this approach using only two quadrature points):

$$\bar{f}(t, x, v) = \omega_1 \delta(v - \mu_1) + \omega_2 \delta(v - \mu_2), \quad (6)$$

where the parameters ω_1 , μ_1 , ω_2 , and μ_2 are all functions of t and x . This approach is reminiscent of other discrete velocity models such as the Broadwell model [2, 3]; however, a key difference is that the discrete velocities, μ_1 and μ_2 , are potentially different at each point in space and time.

The first four moments of (6) are

$$M_0 = \rho = \omega_1 \mu_1^0 + \omega_2 \mu_2^0, \quad (7)$$

$$M_1 = \rho u = \omega_1 \mu_1^1 + \omega_2 \mu_2^1, \quad (8)$$

$$M_2 = \rho u^2 + p = \omega_1 \mu_1^2 + \omega_2 \mu_2^2, \quad (9)$$

$$M_3 = \rho u^3 + 3pu + q = \omega_1 \mu_1^3 + \omega_2 \mu_2^3. \quad (10)$$

If we assume that $\rho > 0$ and $p > 0$, then the above relationship between the moments (M_0, M_1, M_2, M_3) and the parameters $(\mu_1, \mu_2, \omega_1, \omega_2)$ is one-to-one (see discussion below). In the absence of collisions, these moments satisfy equations of the form:

$$M_{\ell,t} + M_{\ell+1,x} = 0 \quad (11)$$

for $\ell = 0, 1, 2, 3$. The moment-closure comes from forcing M_4 to come from (6) (rather than letting it be an independent quantity):

$$M_4 \leftarrow \bar{M}_4 \equiv \int_{-\infty}^{\infty} v^4 \bar{f} dv = \omega_1 \mu_1^4 + \omega_2 \mu_2^4. \quad (12)$$

Therefore, the **moment-closure problem** is reduced to the following: given the first four moments of the system, (M_0, M_1, M_2, M_3) , solve system (7)–(10) to obtain $(\mu_1, \mu_2, \omega_1, \omega_2)$, then use these parameters to calculate \bar{M}_4 via (12).

Solving system (7)–(10) is equivalent to finding the quadrature points and weights for the following weighted Gaussian quadrature rule:

$$\int_{-\infty}^{\infty} g(v) w(v) dv \approx \omega_1 g(\mu_1) + \omega_2 g(\mu_2) \quad (13)$$

with weight function $w(v)$ that satisfies

$$\int_{-\infty}^{\infty} v^k w(v) dv = M_k \quad \text{for } k = 0, 1, 2, 3. \quad (14)$$

If we attempt to make this quadrature rule exact with $g(v) = 1$, v , v^2 , and v^3 , we arrive at equations (7)–(10). To find the correct Gaussian quadrature rule,

we invoke results from classical numerical analysis (e.g., see pages 220-225 of Burden and Faires [4]) and look for polynomials of degree up to two that are orthogonal in the following weighted inner product:

$$\langle g, h \rangle_w := \int_{-\infty}^{\infty} g(v) h(v) w(v) dv. \quad (15)$$

Such polynomials are easily obtained by starting with monomials in v and applying Gram-Schmidt orthogonalization with respect to (15):

$$\psi^{(0)}(v) = 1, \quad (16)$$

$$\psi^{(1)}(v) = v - u, \quad (17)$$

$$\psi^{(2)}(v) = 3\rho p v^2 - (6\rho p u + 3\rho q) v + (3\rho p u^2 - 3p^2 + 3u\rho q). \quad (18)$$

The quadrature points μ_1 and μ_2 are the two distinct real roots of $\psi^{(2)}(v)$:

$$\mu_1, \mu_2 = u + \frac{q}{2p} \mp \sqrt{\left(\frac{p}{\rho} + \left(\frac{q}{2p}\right)^2\right)}. \quad (19)$$

Once the quadrature points are known, the corresponding quadrature weights can easily be obtained by solving equations (7) and (8) for the weights:

$$\omega_1, \omega_2 = \frac{\rho}{2} \pm \frac{\rho^2 q}{2\sqrt{\rho^2 q^2 + 4\rho p^3}}. \quad (20)$$

2.1.1. Flux form of the bi-delta system

Once μ_1 , μ_2 , ω_1 , and ω_2 have been computed, we can evaluate the moment closure: replace the true M_4 with the following:

$$\overline{M}_4 = \mu_1 \omega_1^4 + \mu_2 \omega_2^4 = \rho u^4 + 6pu^2 + 4uq + \frac{q^2}{p} + \frac{p^2}{\rho}. \quad (21)$$

From this we can write down the fully closed system:

$$U_{,t} + F(U)_{,x} = 0, \quad (22)$$

where

$$U = [\rho, \rho u, \rho u^2 + p, \rho u^3 + 3pu + q]^T \quad (23)$$

is the vector of conserved variables and

$$F(U) = \left[\rho u, \rho u^2 + p, \rho u^3 + 3pu + q, \rho u^4 + 6pu^2 + 4uq + \frac{q^2}{p} + \frac{p^2}{\rho} \right]^T \quad (24)$$

is the flux function.

2.1.2. Hyperbolic structure of the bi-delta system

One can show that system (22) with (23)–(24), assuming that $\rho > 0$ and $p > 0$, is a *weakly hyperbolic* system of PDEs. The eigenvalues of the flux Jacobian, F_U , are

$$\lambda^{(1)} = \lambda^{(2)} = \mu_1 \quad \text{and} \quad \lambda^{(3)} = \lambda^{(4)} = \mu_2. \quad (25)$$

The two linearly independent eigenvectors are

$$r^{(1)} = r^{(2)} = [1, \mu_1, \mu_1^2, \mu_1^3]^T \quad \text{and} \quad r^{(3)} = r^{(4)} = [1, \mu_2, \mu_2^2, \mu_2^3]^T. \quad (26)$$

One can show that the simple waves associated with each of these eigenvectors are linearly degenerate:

$$\nabla_U \lambda^{(k)} \cdot r^{(k)} = 0 \quad \text{for} \quad k = 1, 2, 3, 4, \quad (27)$$

where ∇_U is the gradient with respect to the conserved variables (23). For a detailed analysis of this system see Chalons, Kah, and Massot [6].

2.2. Quadrature using Gaussian distributions

There are two main difficulties with moment-closure based on quadrature via delta distributions: (1) the resulting system is only weakly hyperbolic, which means that delta shocks [1, 6, 7] are generically present in the system, and (2) a large number of delta functions may be required to get good agreement with smooth distributions with large support. Yuan and Fox [25] developed an adaptive Gaussian quadrature strategy to help overcome this problem. A possible alternative to using large number of quadrature points was developed Chalons et al. [5] who introduced a quadrature moment-closure based on replacing the Dirac delta functions with Gaussian distribution functions. In particular, in order to simplify the moment inversion equations, each Gaussian is assumed to have the same standard deviation. In the case of two Gaussian distributions this results in an assumed distribution function of the form:

$$\bar{f}(t, x, v) = \frac{\omega_1}{\sqrt{2\pi}\sigma} \exp\left(-\frac{(v - \mu_1)^2}{2\sigma^2}\right) + \frac{\omega_2}{\sqrt{2\pi}\sigma} \exp\left(-\frac{(v - \mu_2)^2}{2\sigma^2}\right), \quad (28)$$

where σ is the width. In the limit as $\sigma \rightarrow 0$ we recover the Dirac delta distribution moment-closure method. In this section we describe the moment-inversion algorithm needed to convert between moments and the parameters in representation (28). Furthermore, we briefly discuss the hyperbolic structure of the resulting evolution equations for the moments of (28).

There are now five free parameters: $(\mu_1, \mu_2, \omega_1, \omega_2, \sigma)$, which can be obtained by solving the following moment-inversion problem on the first five moments:

$$M_0 = \omega_1 \mu_1^0 + \omega_2 \mu_2^0, \quad (29)$$

$$M_1 = \omega_1 \mu_1^1 + \omega_2 \mu_2^1, \quad (30)$$

$$M_2 = \omega_1 \mu_1^2 + \omega_2 \mu_2^2 + \sigma (\omega_1 \mu_1^0 + \omega_2 \mu_2^0), \quad (31)$$

$$M_3 = \omega_1 \mu_1^3 + \omega_2 \mu_2^3 + 3\sigma (\omega_1 \mu_1^1 + \omega_2 \mu_2^1), \quad (32)$$

$$M_4 = \omega_1 \mu_1^4 + \omega_2 \mu_2^4 + 6\sigma (\omega_1 \mu_1^2 + \omega_2 \mu_2^2) + 3\sigma^2 (\omega_1 \mu_1^0 + \omega_2 \mu_2^0). \quad (33)$$

We write this system in terms of primitive variables:

$$\omega_1 \mu_1^0 + \omega_2 \mu_2^0 = \rho, \quad (34)$$

$$\omega_1 \mu_1^1 + \omega_2 \mu_2^1 = \rho u, \quad (35)$$

$$\omega_1 \mu_1^2 + \omega_2 \mu_2^2 = \rho u^2 + \alpha p, \quad (36)$$

$$\omega_1 \mu_1^3 + \omega_2 \mu_2^3 = \rho u^3 + 3\alpha p u + q, \quad (37)$$

$$\omega_1 \mu_1^4 + \omega_2 \mu_2^4 = \rho u^4 + 6\alpha p u^2 + 4q u + r + \frac{3p^2(\alpha^2 - 1)}{\rho}, \quad (38)$$

where we have introduced the parameter α :

$$\sigma = \frac{p}{\rho} (1 - \alpha). \quad (39)$$

We note that the maximum allowable value of α is clearly 1 (otherwise σ would be negative). In fact if $\alpha = 1$, then the bi-Gaussian and the bi-delta function representations are equivalent. What is perhaps less obvious is that the minimum allowed value of α is zero. In fact, as $\alpha \rightarrow 0$, the bi-Gaussian representation collapses into a single Gaussian distribution with width given by the temperature p/ρ . Physically reasonable conditions on the primitive variables guarantee that the α that comes from solving the moment equations (34)–(38) above satisfies $\alpha \in [0, 1]$ (see Theorem 2.1). The exact formula for computing the value of α is given in Algorithm 1.

Theorem 2.1 (Moment-realizability condition). *Assume that the primitive variables satisfy the following conditions:*

- *Positive density:* $0 < \rho$,
- *Positive pressure:* $0 < p$,
- *Lower bound on r :* $\frac{p^3 + \rho q^2}{\rho p} \leq r$,
- *If $q = 0$, bound on r :* $\frac{p^2}{\rho} \leq r \leq \frac{3p^2}{\rho}$.

1. *If $q \neq 0$ then there exists a unique $\alpha \in (0, 1]$ that satisfies the following cubic polynomial:*

$$\mathcal{P}(\alpha) = 2p^3 \alpha^3 + (\rho r - 3p^2) p \alpha - \rho q^2 = 0. \quad (40)$$

Furthermore, from this α we can uniquely obtain the quadrature abscissas and weights in order to exactly solve system (34)–(38):

$$\mu_1, \mu_2 = u + \frac{q}{2p\alpha} \mp \sqrt{\frac{p\alpha}{\rho} + \left(\frac{q}{2p\alpha}\right)^2}, \quad (41)$$

$$\omega_1, \omega_2 = \frac{\rho}{2} \pm \frac{\rho^2 q}{2\sqrt{\rho^2 q^2 + 4\rho p^3 \alpha^3}}. \quad (42)$$

2. If $q = 0$ and $\frac{p^2}{\rho} \leq r < \frac{3p^2}{\rho}$ then there exists a unique $\alpha \in (0, 1]$ such that

$$\alpha = \sqrt{\frac{3p^2 - \rho r}{2p^2}}. \quad (43)$$

Furthermore, in this case the quadrature abscissas (41) and weights (42) are again the unique solutions of system (34)–(38).

3. If $q = 0$ and $r = \frac{3p^2}{\rho}$, then $\alpha = 0$. This case corresponds to a single Gaussian distribution. In this case we lose uniqueness of the quadrature abscissas and weights, but without loss of generality we can take

$$\mu_1, \mu_2 = u, \quad (44)$$

$$\omega_1, \omega_2 = \frac{\rho}{2}, \quad (45)$$

and still exactly solve system (34)–(38).

Proof. We take each point in turn.

1. Let us momentarily assume that α is known and that $\alpha \in (0, 1]$. In this situation we are left with four unknowns: $(\mu_1, \mu_2, \omega_1, \omega_2)$, which are determined by satisfying the first four moment equations: (34)–(37). Just as in the case of quadrature-based moment-closures using delta distributions, these equations can be solved by constructing a set of polynomials that are mutually orthogonal in the inner product (15). The weight function satisfies:

$$\int_{-\infty}^{\infty} v^k w(v) dv = \begin{cases} \rho & \text{if } k = 0, \\ \rho u & \text{if } k = 1, \\ \rho u^2 + \alpha p & \text{if } k = 2, \\ \rho u^3 + 3\alpha p u + q & \text{if } k = 3. \end{cases} \quad (46)$$

Up to degree 2 these mutually orthogonal polynomials can be written as

$$\psi^{(0)}(v) = 1, \quad (47)$$

$$\psi^{(1)}(v) = v - u, \quad (48)$$

$$\psi^{(2)}(v) = v^2 - \left(2u + \frac{q}{p\alpha}\right)v + \left(u^2 + \frac{qu}{p\alpha} - \frac{p\alpha}{\rho}\right). \quad (49)$$

It is easy to show that the two real roots of $\psi^{(2)}(v)$ are (41).

The weights (42) are obtained by plugging (41) into (34) and (35) and solving the resulting 2×2 linear system for ω_1 and ω_2 .

Finally, we must obtain a formula for $\alpha \in (0, 1]$. This is achieved by plugging (41) and (42) into the final moment equation: (38). After simplification this yields the cubic polynomial equation given by (40). We note that under our assumptions we find that

$$\mathcal{P}(0) = -\rho q^2 < 0 \quad \text{and} \quad \mathcal{P}(1) = \rho p \left(r - \frac{p^3 + \rho q^2}{\rho p} \right) \geq 0.$$

Therefore by continuity of $\mathcal{P}(\alpha)$ we are guaranteed that there exists at least one root in $(0, 1]$. To establish that there is a unique root in $(0, 1]$ we note that $\mathcal{P}(\alpha)$ is convex in $(0, 1]$:

$$\mathcal{P}''(\alpha) = 12p^3\alpha > 0 \quad \text{in } (0, 1].$$

The exact formula for computing the value of α is given in Algorithm 1.

2. If $q = 0$ and $\frac{p^2}{\rho} \leq r < \frac{3p^2}{\rho}$ we note that (40) reduces to

$$\mathcal{P}(\alpha) = \alpha(2p^2\alpha^2 + (\rho r - 3p^2)) = 0.$$

The unique root of $\mathcal{P}(\alpha)$ in $(0, 1]$ is given by (43). With this value of α we can again solve (34)–(38) using the μ_1 , μ_2 , ω_1 , and ω_2 given by (41) and (42).

3. If $q = 0$ and $r = \frac{3p^2}{\rho}$ the only solution of (40) is $\alpha = 0$. In this case the moment equations (34)–(38) reduce to

$$M_k = \omega_1\mu_1^k + \omega_2\mu_2^k \quad \text{for } k = 0, 1, 2, 3, 4.$$

This system has an infinite number of solutions of the form:

$$\mu_1 = \mu_2 = u \quad \text{and} \quad \omega_1 + \omega_2 = \rho.$$

Without loss of generality we take (44) and (45).

□

2.2.1. Flux form of the bi-Gaussian system

After obtaining α , μ_1 , μ_2 , ω_1 , and ω_2 , we impose the following moment-closure:

$$\overline{M}_5 = \mu_1\omega_1^5 + \mu_2\omega_2^5 + 10\sigma M_3 - 15\sigma^2 M_1 = \rho u^5 + 10pu^3 + \frac{15p^2u}{\rho} + \alpha\tilde{M}_5, \quad (50)$$

where

$$\tilde{M}_5 = \left(\frac{\tilde{q}^3}{p^2} + \frac{5\tilde{q}^2u}{p} + 10\tilde{q}u^2 + \frac{10p\tilde{q}}{\rho} \right) - \frac{2p\alpha}{\rho} (4\tilde{q} + 5pu), \quad (51)$$

$$\tilde{q} = q/\alpha \quad (\text{we set } \tilde{q} = 0 \text{ if } \alpha = 0). \quad (52)$$

Finally, we write the closed bi-Gaussian quadrature-based moment-closure system in the form (22), where

$$U = [\rho, \rho u, \rho u^2 + p, \rho u^3 + 3pu + q, \rho u^4 + 6pu^2 + 4qu + r]^T, \quad (53)$$

$$F(U) = [\rho u, \rho u^2 + p, \rho u^3 + 3pu + q, \rho u^4 + 6pu^2 + 4qu + r, \overline{M}_5]^T. \quad (54)$$

Algorithm 1 Formula for computing α for the bi-Gaussian closure model (28).

```

1: input:   $(\rho, p, q, r)$ .
2:
3: check:   $\rho > 0, \quad p > 0, \quad r \geq \frac{p^3 + \rho q^2}{\rho p}$ .
4:
5: if  $q = 0$  then
6:   if  $r < \frac{3p^2}{\rho}$  then
7:     return  $\alpha = \sqrt{\frac{3p^2 - \rho r}{2p^2}}$ . // algorithm is finished
8:   else
9:     return  $\alpha = 0$ . // algorithm is finished
10:  end if
11: end if
12:
13: let:   $Q = \frac{1}{6} \left( 3 - \frac{\rho r}{p^2} \right), \quad \mathcal{R} = \frac{\rho q^2}{4p^3}, \quad \mathcal{D} = \mathcal{R}^2 - Q^3$ .
14:
15: if  $\mathcal{D} \geq 0$  then
16:    $\mathcal{T}^* = \mathcal{R} - \sqrt{\mathcal{D}}$ .
17:   if  $\mathcal{T}^* < 0$  then
18:      $\mathcal{T} = -\sqrt[3]{|\mathcal{T}^*|}$ .
19:   else
20:      $\mathcal{T} = \sqrt[3]{\mathcal{T}^*}$ .
21:   end if
22:   return  $\alpha = \sqrt[3]{\mathcal{R} + \sqrt{\mathcal{D}}} + \mathcal{T}$ . // algorithm is finished
23: else
24:    $\theta = \frac{1}{3} \cos^{-1} (\mathcal{R} / \sqrt{Q^3})$ .
25:    $a_1 = 2\sqrt{Q} \cos(\theta)$ .
26:   if  $0 \leq a_1 \leq 1$  then
27:     return  $\alpha = a_1$ . // algorithm is finished
28:   else
29:      $a_2 = 2\sqrt{Q} \cos(\theta + 2\pi/3)$ .
30:     if  $0 \leq a_2 \leq 1$  then
31:       return  $\alpha = a_2$ . // algorithm is finished
32:     else
33:        $a_2 = 2\sqrt{Q} \cos(\theta + 4\pi/3)$ .
34:       return  $\alpha = a_3$ . // algorithm is finished
35:     end if
36:   end if
37: end if

```

2.2.2. Hyperbolic structure of the bi-Gaussian system

The flux Jacobian of the bi-Gaussian system described above can be written in the following form:

$$F_{,U} = \begin{bmatrix} 0 & 1 & 0 & 0 & 0 \\ 0 & 0 & 1 & 0 & 0 \\ 0 & 0 & 0 & 1 & 0 \\ 0 & 0 & 0 & 0 & 1 \\ \overline{M}_{5,M_0} & \overline{M}_{5,M_1} & \overline{M}_{5,M_2} & \overline{M}_{5,M_3} & \overline{M}_{5,M_4} \end{bmatrix}, \quad (55)$$

where $U = (M_0, M_1, M_2, M_3, M_4)^T$ and \overline{M}_5 is given by (50). The eigenvalues and right eigenvectors of the flux Jacobian are of the form

$$\lambda^{(k)} = z_k \quad \text{and} \quad r^{(k)} = [1, z_k, z_k^2, z_k^3, z_k^4]^T, \quad (56)$$

and the left eigenvectors can be written as

$$\ell^{(k)} = \frac{\left[\prod_{j=1}^5 z_j, - \sum_{\substack{j=1 \\ \ell=j+1 \\ m=\ell+1}}^{3,4,5} z_j z_\ell z_m, \sum_{\substack{j=1 \\ \ell=j+1}}^{4,5} z_j z_\ell, - \sum_{j=1}^5 z_j, 1 \right]^T}{\prod_{j=1}^5 (z_k - z_j)}, \quad (57)$$

where all of the above sums and products exclude the index k . Therefore, the eigenstructure hinges on the values of the five numbers: z_k for $k = 1, 2, 3, 4, 5$. Unfortunately, we are not able to obtain these quantities in closed form. However, it is possible to calculate approximate values for these quantities in certain asymptotic limits. In particular, one important limit that is useful later on in this work is the near thermodynamic equilibrium limit, which is characterized here by $\mu_1 \approx \mu_2$. In this limit the five distinct z_k 's are given by

$$z_1, z_2 = u + \frac{2\tilde{q}}{5p} - \sqrt{\frac{(5 \pm \sqrt{10}) p(1 - \alpha)}{\rho}} + \mathcal{O}(|\mu_2 - \mu_1|^2), \quad (58)$$

$$z_3 = u + \frac{2\tilde{q}}{5p} + \mathcal{O}(|\mu_2 - \mu_1|^3), \quad (59)$$

$$z_4, z_5 = u + \frac{2\tilde{q}}{5p} + \sqrt{\frac{(5 \mp \sqrt{10}) p(1 - \alpha)}{\rho}} + \mathcal{O}(|\mu_2 - \mu_1|^2). \quad (60)$$

Assuming that $\rho > 0$ and $p > 0$ and noting that $\alpha \approx 0$ if $\mu_1 \approx \mu_2$, we see that in this limit the system is strongly hyperbolic. We can also approximately compute

$$\nabla_U \lambda^{(k)} \cdot r^{(k)} = \frac{c_k q p^2 (1 - \alpha)^2 (14 p^3 \alpha^3 + 5 \rho q^2)}{20 \rho (4 p^3 \alpha^3 + \rho q^2)^2} + \mathcal{O}(|\mu_2 - \mu_1|^{-2}), \quad (61)$$

where

$$c_k = \left\{ 2 + \sqrt{10}, 2 - \sqrt{10}, \frac{3}{4}, 2 - \sqrt{10}, 2 + \sqrt{10} \right\}.$$

We note that in this limit $\nabla_U \lambda^{(k)} \cdot r^{(k)}$ changes sign if q changes sign, which means that there must exist some state, U^* , for which $\nabla_U \lambda^{(k)} \cdot r^{(k)} = 0$. This shows that the waves in this system are *non-genuinely nonlinear* and may admit composite wave solutions (e.g., see [18]).

In order to illustrate how the bi-Gaussian behaves, we show numerical solutions of two Riemann problems using the discontinuous Galerkin scheme as described in §3.2–§3.3. In Figure 1 we show the solution to a Riemann problem with a heat flux, q , that is strictly positive. In this problem the solution is a set of five classical waves (i.e., shocks and rarefactions). In contrast, in Figure 2 we show the solution to a Riemann problem with heat flux, q , that changes sign over the simulation domain. In this case we see a solution with two compound waves, each of which is a rarefaction connected to a shock, propagating in opposite directions.

2.3. Quadrature using C^0 B-splines

From the above discussion we can view the bi-delta and the bi-Gaussian closure methods as members of the same family of methods, where the bi-delta is one extreme (compactly supported distributions with zero width) and the bi-Gaussian is the other (non-compactly supported distributions with maximal standard deviation as allowed in this representation). Using this point-of-view, we can also construct methods that are in-between these two extremes. One simple example of this is a bi-distribution representation based on C^0 B-splines:

$$\bar{f}(t, x, v) = \omega_1 B_\sigma^0(v - \mu_1) + \omega_2 B_\sigma^0(v - \mu_2), \quad (62)$$

where

$$B_\sigma^0(v) = \begin{cases} \frac{2}{\sigma} (2v + \sqrt{\sigma}) & \text{if } -\sqrt{\sigma} \leq 2v \leq 0, \\ \frac{2}{\sigma} (\sqrt{\sigma} - 2v) & \text{if } 0 \leq 2v \leq \sqrt{\sigma}, \\ 0 & \text{otherwise.} \end{cases} \quad (63)$$

If we introduce the parameter

$$\sigma = \frac{24p}{\rho} (1 - \alpha), \quad (64)$$

and force (62) to have as its first five moments M_0, M_1, M_2, M_3, M_4 , then we again arrive at system (34)–(37), but now with a slightly modified equation to match the M_4 moment:

$$\omega_1 \mu_1^4 + \omega_2 \mu_2^4 = \rho u^4 + 4qu + 6\alpha p u^2 + r + \frac{6p^2}{5\rho} (3\alpha + 2)(\alpha - 1). \quad (65)$$

Theorem 2.2 (Moment-realizability condition). *Assume that the primitive variables satisfy the following conditions:*

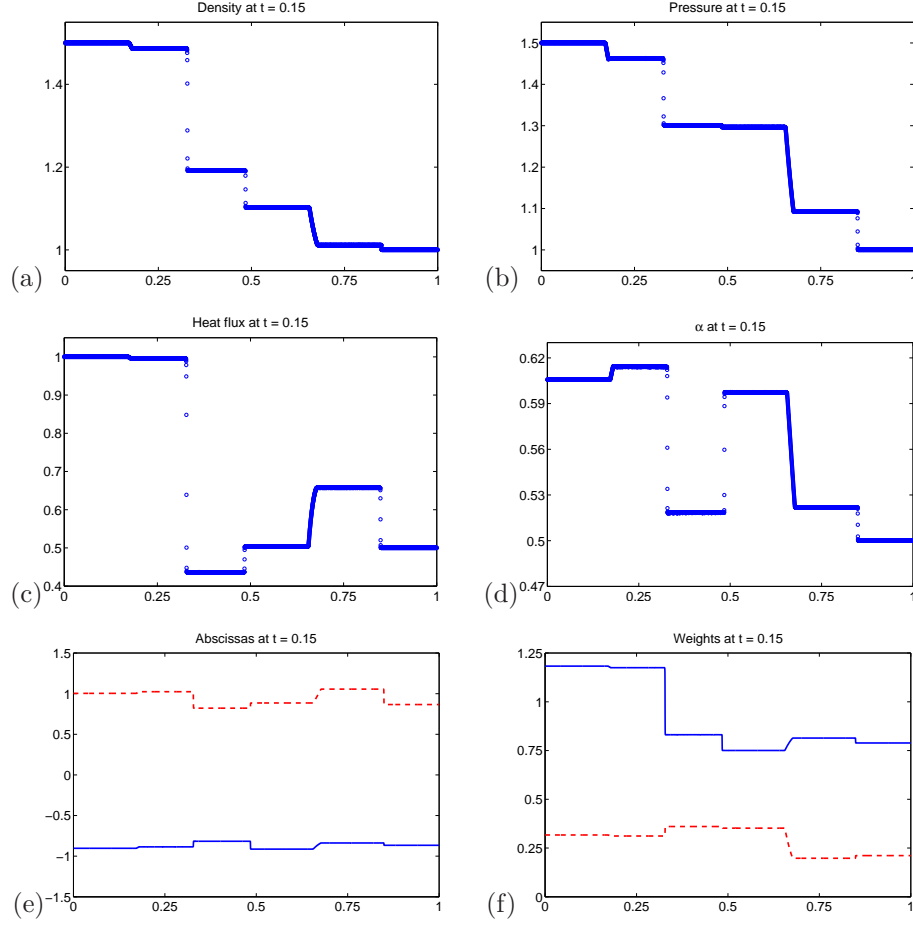


Figure 1: A shock tube problem for the bi-Gaussian system. In this example the initial states are $(\rho, u, p, q, r)_{\text{left}} = (1.5, -0.5, 1.5, 1.0, 4.5)$ and $(\rho, u, p, q, r)_{\text{right}} = (1.0, -0.5, 1.0, 0.5, 3.0)$. This data is chosen so that $q > 0 \forall x, t$, ensuring that we do not encounter points where the convexity changes. Shown in these panels are the (a) density (ρ), (b) pressure (p), (c) heat flux (q), (d) width parameter (α), (e) quadrature abscissas (μ_1, μ_2), and (f) quadrature weights (ω_1, ω_2). The resulting solution shows, counting waves from left to right, a 1-rarefaction, 2-shock, 3-shock, 4-rarefaction, and 5-shock.

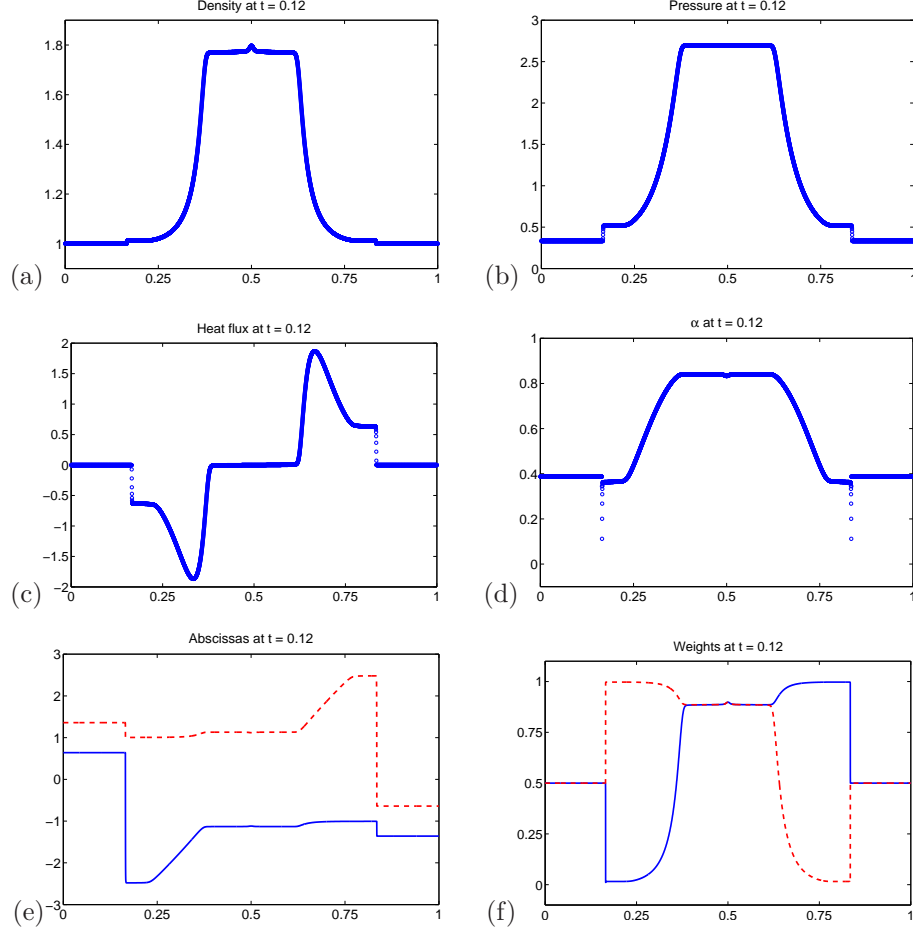


Figure 2: A shock tube problem for the bi-Gaussian system. In this example the initial states are $(\rho, u, p, q, r)_{\text{left}} = (1, 1, 1/3, 0, 0.3)$ and $(\rho, u, p, q, r)_{\text{right}} = (1, -1, 1/3, 0, 0.3)$. This problem is similar to the one shown in Chalons et al. [5]; however, we have reduced the initial value of r from $1/3$ to 0.3 in order to emphasize the 1-shock and 5-shock. Shown in these panels are the (a) density (ρ), (b) pressure (p), (c) heat flux (q), (d) width parameter (α), (e) quadrature abscissas (μ_1, μ_2), and (f) quadrature weights (ω_1, ω_2). The resulting solution shows a 1-shock connected to a 2-rarefaction, as well as a 4-rarefaction connected to a 5-shock. We note that having compound waves is typical of systems with non-convex fluxes (see for example pages 350–357 of LeVeque [16]).

- *Positive density:* $0 < \rho$,
- *Positive pressure:* $0 < p$,
- *Bound on r :* $\frac{q^2}{p} + \frac{p^2}{\rho} \leq r \leq \frac{13q^2}{3p} + \frac{33p^2}{13\rho}$.

Then there exists a unique $\alpha \in [\frac{3}{13}, 1]$ that satisfies the following cubic polynomial:

$$\mathcal{P}(\alpha) = 13p^3\alpha^3 - 6p^3\alpha^2 + \alpha p(5r\rho - 12p^2) - 5\rho q^2 = 0. \quad (66)$$

Using this α and the definitions for the abscissas and weights given by (41) and (42), we can exactly solve the moment inversion problem given by equations (34)–(37) and (65).

Proof. The abscissas and weights given by (41) and (42) automatically satisfy (34)–(37) for any $\alpha \in (0, 1]$. Therefore, the only thing left to do is to satisfy equation (65). Using (41) and (42), one finds that (65) reduces to the cubic polynomial (66). We compute the following:

$$\begin{aligned} \mathcal{P}\left(\frac{3}{13}\right) &= -5\rho q^2 - \frac{495p^3}{169} + \frac{15r\rho p}{13} \leq 0, \quad \mathcal{P}(1) = -5\rho q^2 - 5p^3 + 5r\rho p \geq 0, \\ \text{and } \mathcal{P}''(\alpha) &> 0 \quad \forall \alpha > \frac{2}{13}, \end{aligned}$$

which completes the proof. \square

Remark. Because the bi-B-spline ansatz is compactly supported, there is a maximum value of r that can be represented. In particular, if M_0 through M_4 represent the moments of a Gaussian distribution, the value of $r = 3p^2/\rho$ will exceed the maximum allowed value in the above theorem. In practice we can remedy this situation by taking $\alpha = \frac{3}{13}$ (i.e., the minimum allowed value) whenever r exceeds the maximum allowed value of $\frac{13q^2}{3p} + \frac{33p^2}{13\rho}$.

The moment closure imposed by the bi-B-spline ansatz is the following replacement for the M_5 moment:

$$\begin{aligned} \overline{M}_5 &= \rho u^5 + 10u^2(pu + q) + \frac{2pq}{\rho}(5 - 4\alpha) \\ &\quad + \frac{p^2u}{\rho}(12 + 6\alpha - 13\alpha^2) + \frac{5q^2u}{p\alpha} + \frac{q^3}{p^2\alpha^2}. \end{aligned} \quad (67)$$

The bi-B-spline moment-closure has two advantages over the bi-Gaussian system: (1) α is uniformly bounded away from 0, which means we don't have to worry about the same degeneracies as in the bi-Gaussian case; and (2) the distribution function $\overline{f}(t, x, v)$ is compactly supported and piecewise linear, which makes computing integrals such as those needed in the flux-vector splitting method described in §3.3 simpler. In Figure 3 we show a simulation using the bi-B-spline moment-closure on the same initial data as used in Figure 1.

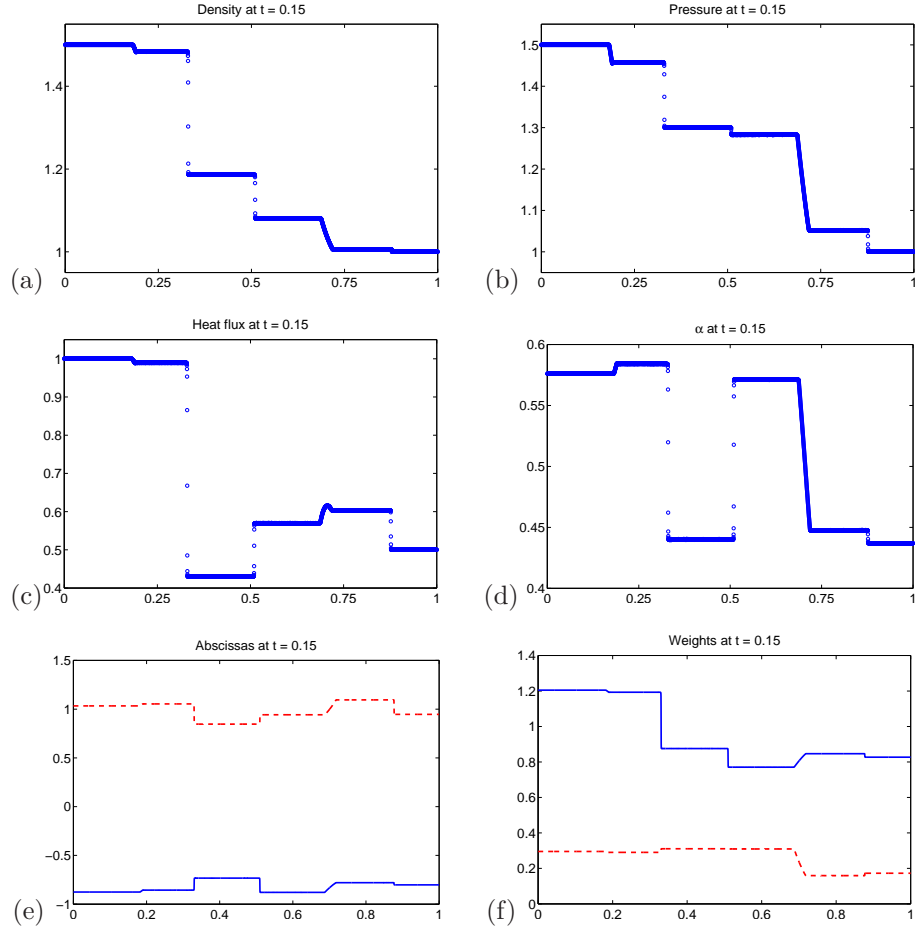


Figure 3: A shock tube problem for the bi-B-spline system. In this example the initial states are $(\rho, u, p, q, r)_{\text{left}} = (1.5, -0.5, 1.5, 1.0, 4.5)$ and $(\rho, u, p, q, r)_{\text{right}} = (1.0, -0.5, 1.0, 0.5, 3.0)$. Shown in these panels are the (a) density (ρ), (b) pressure (p), (c) heat flux (q), (d) width parameter (α), (e) quadrature abscissas (μ_1, μ_2), and (f) quadrature weights (ω_1, ω_2). The resulting solution shows, counting waves from left to right, a 1-rarefaction, 2-shock, 3-shock, 4-rarefaction, and 5-shock.

3. DG quadrature-based moment-closure schemes for VPFP

We describe in this section an application of the quadrature-based moment approach as described in previous sections to a particular set of equations from plasma physics: the Vlasov-Poisson-Fokker-Planck (VPFP) equations (3). Wang and Jin [14] recently developed an *asymptotic-preserving* scheme for the VPFP equation, where they modified a fully kinetic solver for VPFP so that it remains asymptotic preserving in the high-field limit $\varepsilon \rightarrow 0^+$. Although the Wang and Jin approach has the nice property that it can be applied for *any* value of $\varepsilon > 0$, if one is really interested in regimes where ε is relatively small (i.e., *near* thermodynamic equilibrium), then their approach is computationally expensive (i.e., requires solving a PDE in 2D rather than 1D). Our focus in this section is on approximately solving the VPFP system using quadrature-based moment-closure techniques that remain asymptotic-preserving in the high-field limit $\varepsilon \rightarrow 0^+$. This approach allows us to efficiently capture *near* thermodynamic equilibrium solutions.

3.1. Strang operator splitting

Wang and Jin [14] achieve an asymptotic-preserving scheme through the use of a clever semi-implicit time discretization. In this work we make use of a more standard trick: Strang operator splitting [24], which has been used for Vlasov-Poisson simulations since the work of Cheng and Knorr [8]. In particular, Schaeffer [23] modified the Cheng and Knorr approach to construct an efficient method for VPFP.

In our approach we use a Strang splitting for the VPFP system under a quadrature-based moment-closure with the following steps:

1. Solve the Poisson equation:

$$-\phi_{,x,x} = \rho_0(x) - \rho^n(x), \quad E^n = -\phi_{,x}.$$

2. On $[t^n, t^n + \frac{\Delta t}{2}]$ and for $\ell = 0, 1, 2, 3, 4$ solve VPFP with only the collision operator ($M^n \rightarrow \widetilde{M}^n$):

$$M_{\ell,t} = \frac{1}{\varepsilon} \{ \ell(\ell-1)M_{\ell-2} - \ell E^n M_{\ell-1} - \ell M_{\ell} \}.$$

3. On $[t^n, t^n + \Delta t]$ solve the *collisionless* quadrature-based moment-closure system (22) with the appropriate definitions for U and $F(U)$ ($\widetilde{M}^n \rightarrow \widetilde{M}^{n+1}$).

4. Solve the Poisson equation:

$$-\phi_{,x,x} = \rho_0(x) - \widetilde{\rho}^{n+1}(x), \quad \widetilde{E}^{n+1} = -\phi_{,x}.$$

5. On $[t^n + \frac{\Delta t}{2}, t^n + \Delta t]$ and for $\ell = 0, 1, 2, 3, 4$ solve VPFP with only the collision operator ($\widetilde{M}^{n+1} \rightarrow M^{n+1}$):

$$M_{\ell,t} = \frac{1}{\varepsilon} \left\{ \ell(\ell-1)M_{\ell-2} - \ell\widetilde{E}^{n+1}M_{\ell-1} - \ell M_{\ell} \right\}.$$

The spatial discretizations are handled via a high-order discontinuous Galerkin discretization, which is briefly described below.

3.2. High-order discontinuous Galerkin spatial discretization

We make use of the discontinuous Galerkin (DG) method as developed by Cockburn and Shu [9] and implemented in the **DoGPack** software package [21] to solve hyperbolic conservations of the form (22).

We begin by constructing an equally spaced numerical grid on $[a, b]$ consisting of M elements, each of the form: $\mathcal{T}_i = [x_i - \frac{\Delta x}{2}, x_i + \frac{\Delta x}{2}]$, where $\Delta x = (b - a)/M$ is the grid spacing. Note that x_i denotes the center of element \mathcal{T}_i . Next we define the *broken* finite element space

$$\mathcal{V}^{\Delta x} = \{v^{\Delta x} \in L^\infty(\Omega) : v^{\Delta x}|_{\mathcal{T}_i} \in P^k \forall i\}, \quad (68)$$

meaning that on each element \mathcal{T}_i , $v^{\Delta x}$ will be a polynomial of degree at most k . The solution, $U^{\Delta x} \in \mathcal{V}^{\Delta x}$, restricted to element \mathcal{T}_i can be written as

$$U^{\Delta x}|_{\mathcal{T}_i} = \sum_{\ell=1}^k U^\ell(t) \varphi_\ell(\xi), \quad (69)$$

where on each element $x = x_i + \xi (\Delta x/2)$, and $\varphi(\xi)$ are the orthonormal Legendre polynomials:

$$\varphi(\xi) = \left\{ 1, \sqrt{3}\xi, \frac{\sqrt{5}}{2}(3\xi^2 - 1), \dots \right\}. \quad (70)$$

In order to obtain the semi-discrete DG method we multiply (22) by $\varphi_j(\xi)$, integrate over a single element \mathcal{T}_i , replace the exact U by (69), and integrate-by-parts in x . After simplification, this results in the following set of coupled ordinary differential equations in time:

$$\frac{d}{dt} U_i^j = \frac{1}{\Delta x} \int_{-1}^1 F(U) \varphi_{j,\xi} d\xi - \frac{1}{\Delta x} \left[\varphi_j(1) \mathcal{F}_{i+\frac{1}{2}} - \varphi_j(-1) \mathcal{F}_{i-\frac{1}{2}} \right], \quad (71)$$

where $\mathcal{F}_{i-\frac{1}{2}}$ is the *numerical flux* at interface $x = x_{i-\frac{1}{2}}$, which must be calculated from an (approximate) Riemann solver (see §3.3 below). In order to time advance this semi-discrete scheme, we make use of the standard third-order total variation diminishing Runge-Kutta (TVD-RK) as described in Gottlieb and Shu [12]. We make use of the moment-limiters described in Krivodonova [15] to suppress unphysical oscillations when required.

Finally we note that the Poisson equation in the operator split scheme described above is solved using a local discontinuous Galerkin scheme that is described in detail in Rossmanith and Seal [22].

3.3. Kinetic-based Riemann solvers

One missing ingredient from the discussion of the discontinuous Galerkin scheme in the previous section is a description of how the numerical flux, $\mathcal{F}_{i-\frac{1}{2}}$, is computed. Since we have the ability to reconstruct the distribution function $\bar{f}(t, x, v)$ for any (t, x) , we can use a kinetic flux-vector splitting approach (see for example Mandal and Deshpande [19]). In kinetic flux-vector splitting we split the flux into right-going contributions immediately to the left of interface $x_{i-\frac{1}{2}}$ and left-going contributions immediately to the right of interface $x_{i-\frac{1}{2}}$:

$$\mathcal{F}_{i-\frac{1}{2}} = \mathcal{F}_{i-\frac{1}{2}}^+ + \mathcal{F}_{i-\frac{1}{2}}^-, \quad (72)$$

where

$$\mathcal{F}_{i-\frac{1}{2}}^+ = \int_0^\infty \bar{f}(t, x_{i-\frac{1}{2}}^-, v) dv \quad \text{and} \quad \mathcal{F}_{i-\frac{1}{2}}^- = \int_{-\infty}^0 \bar{f}(t, x_{i-\frac{1}{2}}^+, v) dv. \quad (73)$$

3.4. Stiff source term solution and the asymptotic-preserving condition

The final missing part of the Strang operator split algorithm presented in §3.1 is the solver for the collision operator. A big advantage of considering fluid solvers over kinetic solvers in the context of VPFP is that the diffusion operator in v becomes an ODE for the moments. In particular, in the Strang split approach detailed in §3.1, the electric field, $E(t, x)$, is frozen in time during each of the collision operator steps, meaning that the resulting ODEs are linear constant coefficient equations that can easily be solved exactly. The full solution over a time step $[t^n, t^n + \Delta t]$ with initial data $(M_0^n, M_1^n, M_2^n, M_3^n, M_4^n)$ is

$$M_0^{n+1} = M_0^n, \quad (74)$$

$$M_1^{n+1} = Z(EM_0^n + M_1^n) - EM_0^n, \quad (75)$$

$$M_2^{n+1} = Z^2((E^2 - 1)M_0^n + 2EM_1^n + M_2^n) - 2EZ(EM_0^n + M_1^n) + (1 + E^2)M_0^n, \quad (76)$$

$$M_3^{n+1} = Z^3(E(E^2 - 3)M_0^n + 3(E^2 - 1)M_1^n + 3EM_2^n + M_3^n) - 3EZ^2((E^2 - 1)M_0^n + 2EM_1^n + M_2^n) + 3(E^2 + 1)Z(EM_0^n + M_1^n) - E(E^2 + 3)M_0^n, \quad (77)$$

$$M_4^{n+1} = Z^4((E^4 - 6E^2 + 3)M_0^n + 4E(E^2 - 3)M_1^n + 6M_2^n(E^2 - 1) + 4EM_3^n + M_4^n) - 4EZ^3(E(E^2 - 3)M_0^n + 3M_1^n(E^2 - 1) + 3EM_2^n + M_3^n) + 6(E^2 + 1)Z^2((E^2 - 1)M_0^n + 2EM_1^n + M_2^n) - 4E(E^2 + 3)Z(EM_0^n + M_1^n) + (E^4 + 6E^2 + 3)M_0^n, \quad (78)$$

where $E = E^n$ and $Z = \exp[-\Delta t/\varepsilon]$.

4. Numerical simulations in the high-field limit

In order to verify the proposed DG operator split method using the quadrature-based moment-closure we consider two test cases from Wang and Jin [14]: (1) verification of the asymptotic-preserving property and (2) a periodic Riemann problem. All of these problems are defined on $[0, 1]$ with periodic boundary conditions.

4.1. Verification of the asymptotic-preserving property

In order to verify the asymptotic-preserving property of the proposed scheme, we attempt two versions of the same problem from Wang and Jin [14].

For the first problem we start with an isothermal Gaussian:

$$f(0, x, v) = \frac{\rho(0, x)}{\sqrt{2\pi}} \exp \left[-\frac{1}{2} (v + E(0, x))^2 \right], \quad (79)$$

$$\rho(0, x) = \frac{\sqrt{2\pi}}{2} (2 + \cos(2\pi x)). \quad (80)$$

with a neutralizing background charge of

$$\rho_0(x) = \frac{\sqrt{2\pi}}{1.2660658777520083} \exp[\cos(2\pi x)]. \quad (81)$$

The quantity $\|M_1 + \rho E\|_{L^2}$ is plotted for various ε as a function of time in Figure 4(a). These results verify that $\|M_1 + \rho E\|_{L^2} = \mathcal{O}(\varepsilon)$ for all t .

For the second problem we start with initial data that is not in isothermal equilibrium:

$$f(0, x, v) = \frac{\rho(0, x)}{2\sqrt{2\pi}} \left(\exp \left[-\frac{1}{2} (v + 1.5)^2 \right] + \exp \left[-\frac{1}{2} (v - 1.5)^2 \right] \right), \quad (82)$$

with the same $\rho(0, x)$ and neutralizing background charge as in the previous example. The quantity $\|M_1 + \rho E\|_{L^2}$ is plotted for various ε as a function of time in Figure 4(b). These results verify that the numerical schemes immediately drives the non-equilibrium initial data near the equilibrium distribution such that $\|M_1 + \rho E\|_{L^2} = \mathcal{O}(\varepsilon)$.

The simulations presented in Figure 4 were done with the bi-Gaussian moment-closure. The bi-delta and bi-B-spline methods give near identical results for this problem.

4.2. Double periodic Riemann problem

The initial data is the distribution function (79) with

$$(\rho(0, x), \rho_0(x)) = \begin{cases} (1/8, 1/2) & \text{if } 0 \leq x < 1/4, \\ (1/2, 1/8) & \text{if } 1/4 \leq x < 3/4, \\ (1/8, 1/2) & \text{if } 3/4 \leq x \leq 1. \end{cases} \quad (83)$$

The solution using the bi-B-spline moment-closure is shown in Figure 5. The results agree well with those in Wang and Jin [14]. The bi-Gaussian moment-closure has difficulties with this problem due to the steep gradients in the solution in regions where α is small but non-zero.

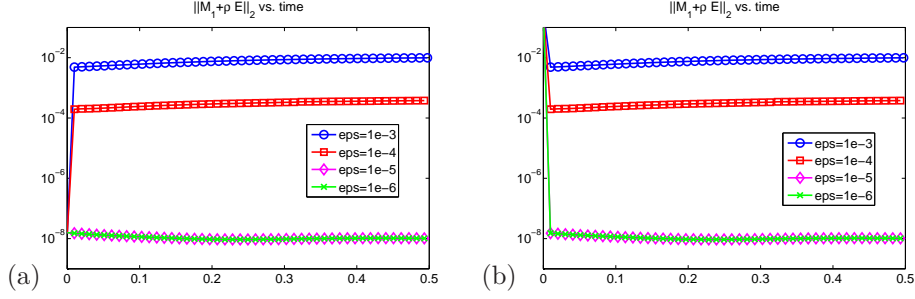


Figure 4: Verification of the asymptotic preserving capability of the method. Shown in these two plots are the L^2 -norms of the difference in the fluid mean velocity (u) and the equilibrium mean velocity ($-\rho E$) as a function of time. In Panel (a) the initial conditions are already in equilibrium, while in Panel (b) the initial conditions is not in equilibrium. We show only every 20th time step value so that the various curves are more easily identified. We note that for $\epsilon = 10^{-5}$ and $\epsilon = 10^{-6}$, the resolution in the simulations is not enough to resolve the non-equilibrium deviations; and therefore, the difference between u and $-\rho E$ is negligible. All runs were done with 64 mesh elements.

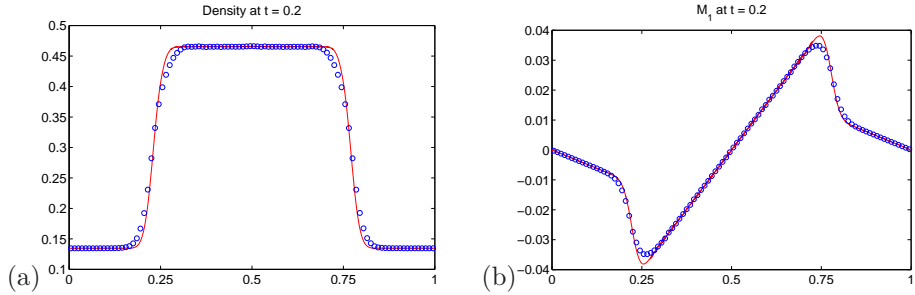


Figure 5: Periodic Riemann problem of Wang and Jin [14]. Shown are the solutions with 100 elements (blue circles) and 2000 elements (red line). This simulation is difficult for the bi-Gaussian moment-closure due to the steep gradients in the solution in regions where α is small but non-zero. These simulations were instead done with the bi-B-spline moment-closure and the results show good agreement with the results of Wang and Jin [14].

5. Summary

In this work we considered quadrature-based moment-closure methods using two quadrature points. We briefly investigated the properties of these methods and showed connections between bi-delta, bi-Gaussian, and bi-B-spline quadrature methods. We then applied this formulation to the Vlasov-Poisson-Fokker-Planck system in the high-field limit, and, using a high-order discontinuous Galerkin scheme with Strang operator splitting, verified the scheme on two test problems. Future work will focus on multidimensional plasma physics applications.

Acknowledgements. This work was supported in part by NSF grant DMS-1016202.

References

- [1] F. Bouchut. On zero pressure gas dynamics. In *Advances in Kinetic Theory and Computing*, volume 22, pages 171–190. World Scientific, 1994.
- [2] J.E. Broadwell. Shock structure in a simple discrete velocity gas. *Phys. Fluids*, 7:1243–1247, 1964.
- [3] J.E. Broadwell. Study of rarefied shear flow by the discrete velocity method. *J. Fluid Mech.*, 19:401–414, 1964.
- [4] R.L. Burden and J.D. Faires. *Numerical Analysis*. Thomson Brooks/Cole, 8th edition, 2005.
- [5] C. Chalons, R.O. Fox, and M. Massot. A multi-Gaussian quadrature method of moments for gas-particle flows in a LES framework. In *Proceedings of the Summer Program*, pages 347–358. Center for Turbulence Research, 2010.
- [6] C. Chalons, D. Kah, and M. Massot. Beyond pressureless gas dynamics: Quadrature-based velocity moment models. *Comm. Math. Sci.*, 10:1241–1272, 2012.
- [7] G.-Q. Chen and H. Liu. Formation of δ -shocks and vacuum states in the vanishing pressure limits of solutions to the euler equations. *SIAM J. Math. Anal.*, 34:923–938, 2003.
- [8] C. Cheng and G. Knorr. The integration of the Vlasov equation in configuration space. *J. Comp. Phys.*, 22:330–351, 1976.
- [9] B. Cockburn and C.-W. Shu. Runge-Kutta discontinuous Galerkin methods for convection-dominated problems. *J. Sci. Comput.*, 16:173–261, 2001.
- [10] R.O. Fox. Higher-order quadrature-based moment methods for kinetic equations. *J. Comp. Phys.*, 228:7771–7791, 2009.

- [11] L. Gosse, S. Jin, and X. Li. Two moment systems for computing multiphase semiclassical limits of the Schrödinger equation. *Math. Models Methods Appl. Sci.*, 13:1689–1723, 2003.
- [12] S. Gottlieb and C.-W. Shu. Total variation diminishing Runge-Kutta schemes. *Math. of Comput.*, 67:73–85, 1998.
- [13] S. Jin and X. Li. Multi-phase computations of the semiclassical limit of the Schrödinger equation and related problems: Whitham vs. Wigner. *Phys. D*, 182:46–85, 2003.
- [14] S. Jin and L. Wang. An asymptotic preserving scheme for the Vlasov-Poisson-Fokker-Planck system in the high field regime. *Acta Math. Sci.*, 31B:2219–2232, 2011.
- [15] L. Krivodonova. Limiters for high-order discontinuous Galerkin methods. *J. Comp. Phys.*, 226:879–896, 2007.
- [16] R.J. LeVeque. *Finite Volume Methods for Hyperbolic Problems*. Cambridge University Press, 2002.
- [17] X. Li, J.G. Wöhlbier, S. Jin, and J.H. Booske. An Eulerian method for computing multi-valued solutions of the Euler-Poisson equations and applications to wave breaking in klystrons. *Phys. Rev. E*, 70(016502), 2004.
- [18] T.P. Liu. The Riemann problem for general 2×2 conservation laws. *Trans. Amer. Math. Soc.*, 199:89–112, 1974.
- [19] J.C. Mandal and S.M. Deshpande. Kinetic flux vector splitting for euler equations. *Comput. Fluids*, 23:447–478, 1994.
- [20] J. Nieto, F. Poupaud, and J. Soler. High-field limit for the Vlasov-Poisson-Fokker-Planck system. *Arch. Ration. Mech. Anal.*, 158:20–59, 2001.
- [21] J.A. Rossmannith. DoGPACK: Discontinuous Galerkin Package. <http://www.dogpack-code.org>.
- [22] J.A. Rossmannith and D.S. Seal. A positivity-preserving high-order semi-Lagrangian discontinuous Galerkin scheme for the Vlasov-Poisson equations. *J. Comp. Phys.*, 230:6203–6232, 2011.
- [23] J. Schaeffer. Convergence of a difference scheme for the Vlasov-Poisson-Fokker-Planck system in one dimension. *SIAM J. Numer. Anal.*, 35:1149–1175, 1998.
- [24] G. Strang. On the construction and comparison of difference schemes. *SIAM J. Numer. Anal.*, 5:506–517, 1968.
- [25] C. Yan and R.O. Fox. Conditional quadrature method of moments for kinetic equations. *J. Comp. Phys.*, 230:8216–8246, 2011.